Relative Yields of Neutron Groups from the $Li^7(p,n)Be^7$, Be^{7*} Reactions*

P. R. BEVINGTON, W. W. ROLLAND,† AND H. W. LEWIS‡
Duke University, Durham, North Carolina

(Received September 23, 1960)

The relative yields of the two groups of neutrons from the $Li^7(p,n)Be^7$, Be^{7*} reaction, leading to the ground state and the 430-kev state of Be^7, have been measured with a time-of-flight system, using pre-acceleration pulsing of the accelerator beam. Data were taken at 30° intervals between 0° and 150° for proton energies high enough to produce (p,n') neutrons above the detection threshold (300 kev). Since the yield of the (p,n) reaction is more highly peaked in the forward direction than that of the (p,n') reaction, the ratio of the (p,n') to (p,n) intensities grows with increasing angle, severely limiting the usefulness of the (p,n) reaction as a neutron source above the (p,n') threshold at back angles. Absolute differential and total cross sections for both groups have been calculated from the data. A comparison with theory for total cross sections and angular distributions suggests the existence of three previously unidentified levels in Be^8. One level, with $J^\pi=1^-$, near the threshold for the (p,n') reaction, is responsible for the fast rise in the (p,n') total cross section near threshold. A second level, corresponding to an incident proton energy of about 3.0 Mev, does not contribute significantly to the yield of the (p,n') reaction; the data are consistent with an assignment of $J^\pi=1^+$ and a total width of 1 Mev. The bulk of the total cross-section curve for the (p,n') reaction has been fitted by assuming a 1^+ level corresponding to an incident proton energy of 3.5 Mev, with $\gamma_n^2 \simeq \gamma_p^2$, $\gamma_{n'}^2 \simeq 5\gamma_{p'}^2$, and $\gamma_{p'}^2 \ll \gamma_p^2$.

THE $Li^7(p,n)Be^7$ reaction is a widely used source of monoenergetic neutrons and has therefore been studied in detail from threshold, at a proton energy of 1.881 Mev, to a proton energy of 2.378 Mev. Above the latter energy, however, a second group of neutrons emerges, leading to the first excited state of Be^7 at 430 kev. No systematic study of the neutron yields has been made for proton energies above 2.87 Mev[1,2] except measurements of the total cross section for production of all neutrons[3] and the 0° differential cross section for production of all neutrons.[4,5]

A knowledge of the relative intensities of the two groups is important in experiments requiring monoenergetic neutrons with energies above 650 kev. Furthermore, the levels excited in the compound nucleus Be^8 are sufficiently separated that some of the parameters of these levels may be calculated from angular distributions and total cross sections for the two groups.

In the present experiment[6] the relative yields of the two groups were measured at 30° intervals from 0° to 150° (laboratory angle) for bombarding energies high enough to produce (p,n') neutrons above the effective detection threshold (300 kev). Measurements were made in 100-kev and 200-kev steps up to the maximum proton energy available, 4.1 Mev.

EXPERIMENTAL METHOD

The data were taken with a time-of-flight system utilizing a pulsed proton beam and a time-to-pulse-height converter of Los Alamos design.[7] Neutrons from the lithium target were detected with a plastic scintillator viewed by two photomultiplier tubes in fast coincidence. The timing signal, denoting the production time of the neutrons, was derived from the instantaneous voltage of the target.

Proton bursts approximately 6 nsec long, separated by 200 nsec, were produced in the high-voltage terminal of the Duke University 4-Mv Van de Graaff accelerator. The proton source was adapted from an Oak Ridge design[8–10] and incorporated a strong-focusing *einzel* lens followed by a gap lens. To pulse the proton beam the focused image of the *einzel* lens was swept past the object aperture of the gap lens by a 5-Mc/sec sinusoidal voltage applied to a pair of deflecting plates near the probe canal of the rf ion source. A similar pair of deflecting plates near the gap lens aperture, with a small steady voltage between them, refracted the two ion bursts per cycle asymmetrically so that one burst was removed from the beam while the other was refracted onto the axis of the accelerator.[11,12]

The target, a thin layer of metallic lithium evaporated onto a tantalum end cap 0.010 in. thick, was electrically insulated from the beam pipe by a glass tube with a wall thickness of 2 mm. Voltage pulses caused by the charging of the target capacitance by the proton bursts were capacitively coupled to a distributed amplifier, while the averaged current passed into a current integrator. To stabilize the capacitance of the target and to prevent pickup, the target was surrounded by a grounded copper shield consisting of a

* This work was supported by the U. S. Atomic Energy Commission.

† Now at Kings College, Bristol, Tennessee.

‡ Currently on leave at American University of Beirut, Beirut, Lebanon.

[1] R. Batchelor, Proc. Phys. Soc. (London) **A68**, 452 (1955).

[2] R. Batchelor and G. C. Morrison, Proc. Phys. Soc. (London) **A68**, 1081 (1955).

[3] J. H. Gibbons and R. L. Macklin, Phys. Rev. **114**, 571 (1959).

[4] J. K. Bair *et al.*, Phys. Rev. **85**, 946 (1952).

[5] F. Gabbard, R. H. Davis, and T. W. Bonner, Phys. Rev. **114**, 201 (1959).

[6] P. R. Bevington, G. E. Mitchell, W. W. Rolland, R. M. Wilenzick, and H. W. Lewis, Bull. Am. Phys. Soc. 4, 218 (1959).

[7] W. Weber, C. W. Johnstone, and L. Cranberg, Rev. Sci. Instr. **27**, 166 (1956).

[8] C. H. Johnson, J. P. Judish, and C. W. Snyder, Rev. Sci. Instr. **28**, 942 (1957).

[9] V. E. Parker and R. F. King, Bull. Am. Phys. Soc. **1**, 70 (1956).

[10] We are indebted to Dr. J. H. Gibbons for sending us drawings of the Oak Ridge source.

[11] C. M. Turner and S. D. Bloom, Rev. Sci. Instr. **29**, 480 (1958).

[12] H. W. Lewis, P. R. Bevington, W. W. Rolland, R. L. Rummel, and R. M. Wilenzick, Rev. Sci. Instr. **30**, 923 (1959).

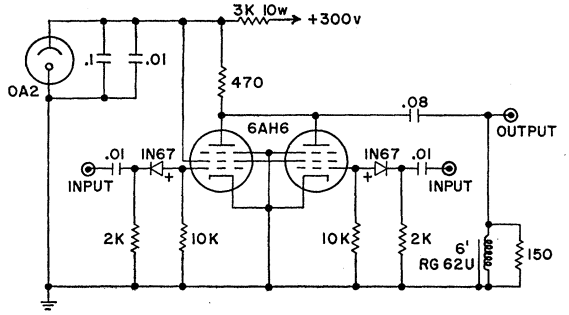

FIG. 1. Fast coincidence circuit to supply the "start" input to time-to-pulse-height converter.

cylinder 5 in. in diameter and 8 in. long with a wall thickness of 0.010 in.

The timing signal from the target was fed to a tuned 5-Mc/sec amplifier[12] to produce a sinusoidal signal for the "stop" input of the time-to-pulse-height converter. A 0°–360° phase shifter incorporated in the tuned amplifier provided a variable time delay between the "start" pulses from the scintillator and the "stop" pulses to permit a shifting of the positions of peaks in the time spectrum from the converter as displayed on a 100-channel pulse-height analyzer.

The lithium target was 35 kev thick to protons at an energy of 1.89 Mev. Proton energies were calculated from a potentiometer reading of the accelerator's generating voltmeter, which was calibrated repeatedly at the $Li^7(p,n)$ threshold and later compared with an electrostatic analyzer for linearity.

The neutron detector consisted of a plastic scintillator 2 in. square and 1 in. thick to the neutron beam, optically coupled to two RCA 6342 photomultiplier tubes. The entire assembly was mechanically connected and optically shielded by a lead cylinder with a wall thickness of $\frac{3}{16}$ in., extending to the Bakelite bases of the tubes. The detector was shielded from room-scattered neutrons by a collimator similar to that used by Cranberg *et al.*[13,14]

Pulses from each photomultiplier tube were fed through two distributed amplifiers into the fast coincidence circuit shown in Fig. 1. This circuit effectively eliminated noise pulses from the photomultiplier tubes. Pulse shaping to overcome ringing from the distributed amplifiers was accomplished by diodes in the grid circuits which stretched the pulses without altering their rise times. The resolving time of the coincidence circuit was about 15 nsec, with a doubles-to-singles amplitude ratio of two to one for negative input pulses of 3 v or more. The output pulses were amplified and inverted by a distributed amplifier before being fed to the input of the time-to-pulse-height converter.

Input pulses which do not cut off the coincidence tubes completely can produce immature output pulses which trigger the converter late. To remove this source of time spread the output pulses from the coincidence circuit were amplified and then applied as a biased gate to the multichannel analyzer.

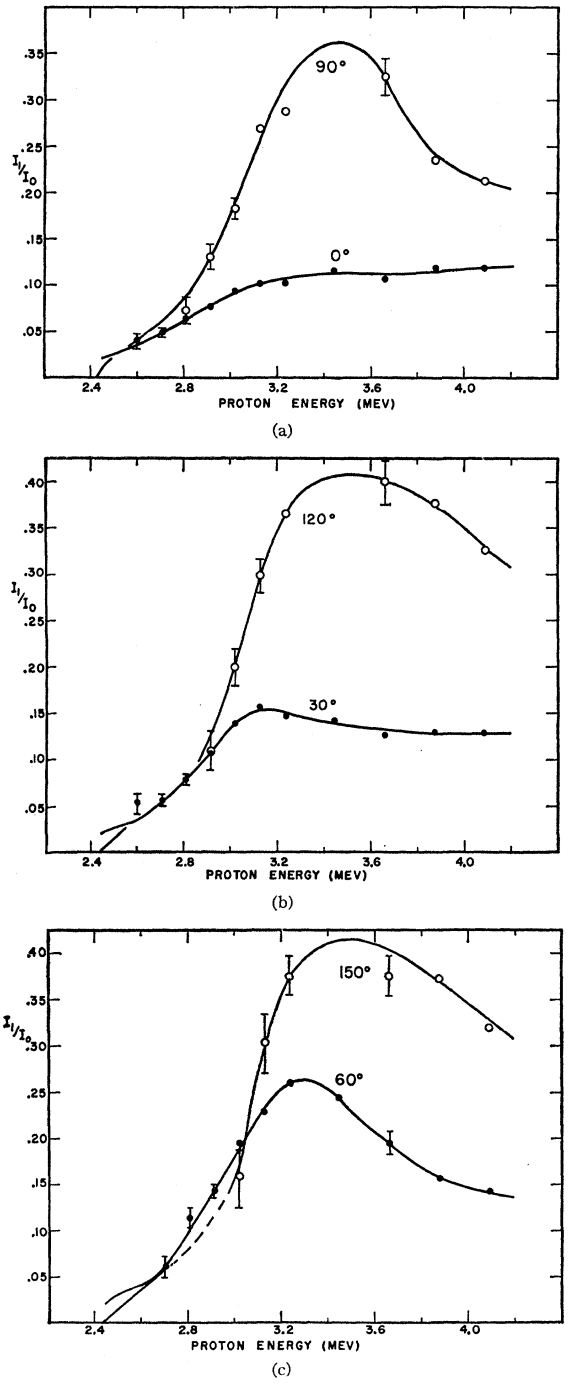

FIG. 2. Ratios of the intensities of the neutron groups from the $Li^7(p,n')Be^{7*}$ and $Li^7(p,n)Be^7$ reactions. Low-energy extrapolations are derived from those for the differential cross sections shown in Figs. 3 and 4.

[13] L. Cranberg, R. K. Beauchamp, and J. S. Levin, Rev. Sci. Instr. **28**, 89 (1957).

[14] Li_2CO_3 supplied free by American Potash and Chemical Corporation.

All measurements were monitored by a McKibben long counter at an angle of 60° with respect to the proton beam. The efficiency of this counter was considered to be flat over the energy range of the experiment. Corrections were made to the data for absorption of neutrons by air, copper, glass, and tantalum surrounding the target, but these corrections were less than 3%. The data were taken in three short consecutive runs, with a relative (as a function of energy) efficiency measurement of the neutron detection system for each run.

To measure efficiency the scintillator was placed at 60° (opposite to the position of the long counter) at the same distance from the target (increased in successive runs to resolve progressively more energetic neutron groups) as that at which the data were taken. Time-of-flight spectra were then taken at proton energy intervals of 50 kev or 100 kev over the desired energy range for a preset number of counts from the long counter. The scintillator counted the two neutron groups separately with different efficiencies, whereas the McKibben monitor counted the total number of neutrons emitted at 60° in both groups. The detector efficiency was therefore calculated from the yield of the (p,n) reaction only, correcting the monitor counts by multiplying by the ratio at 60° of the yield of the (p,n) reaction to the total neutron yield: $I_0(60°)/I(60°)$, where I_0 and I_1 are the neutron intensities from the (p,n) and (p,n') reactions, respectively, and $I=I_0+I_1$. This ratio was determined by an iterative procedure of applying an estimated efficiency to the final data to find a value for the ratio and using this value to find a better estimate of the efficiency, and so on. It should be noted that this iterative procedure is valid only because efficiency measurements were made for proton energies below the threshold for the (p,n') reaction.

At high neutron energies the efficiency curve approaches the shape of the n-p scattering cross section and the efficiency is quite stable. For low-energy neutrons (below about 250 kev) the efficiency rises sharply with increasing energy as a larger portion of the white spectrum from the scintillator is detected, and the shape of the curve is very sensitive to small changes in photomultiplier tube or distributed amplifier gain. Therefore, even though detection is possible for neutrons emitted at the $Li^7(p,n)$ threshold (about 30 kev), the slow fluctuation of efficiency with time was prohibitive for neutrons with less than 300-kev energy, the effective lower limit for detection.

RESULTS

The ratios I_1/I_0 of the intensities of the (p,n') and (p,n) neutron groups are shown in Fig. 2. Errors for the two lowest energy points at each angle are ±20% and ±10%, respectively, because of uncertainties in efficiency measurements; for all other points the errors are ±6%, as shown. Solid curves are drawn through the data points, except that the extrapolations below 2.7 Mev are calculated from the results of Batchelor and Morrison[2] (see below) for the (p,n') reaction and from an extrapolation of our results for the (p,n) reaction. The shapes of the curves at back angles for proton energies near 3.4 Mev are inferred from interpolation of the differential cross-section curves for the two groups.

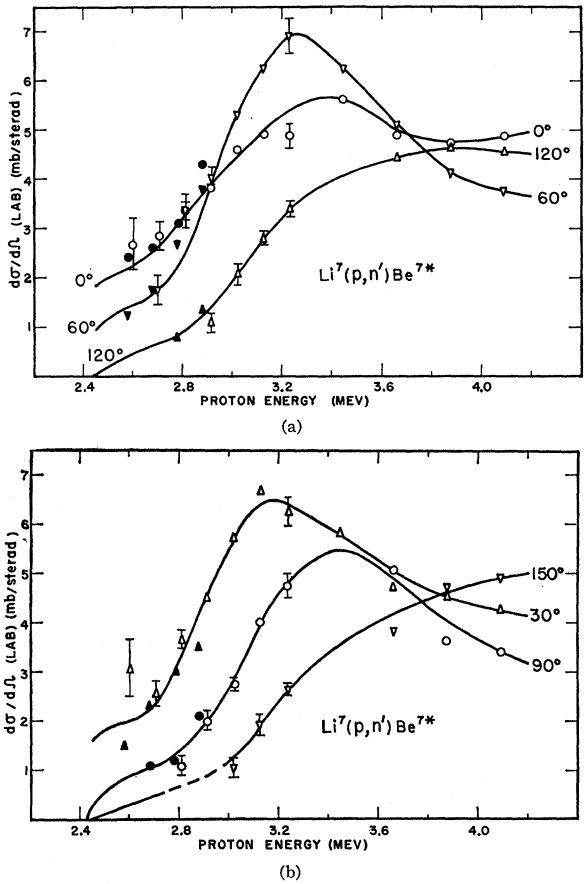

FIG. 3. Differential cross sections of the (p,n') reaction, normalized to the 0° cross section of Gabbard *et al.*[5] Solid dots are from the work of Batchelor and Morrison[2] and low-energy extrapolations are calculated from their (p,n') total cross section, assuming isotropy in the center-of-mass system.

The absolute differential cross section $\sigma_i(\theta)$ at angle θ for each group is obtained by multiplying the ratio $I_i(\theta)/I(0°)$ by the 0° absolute differential cross section for the sum of the two groups as measured by Gabbard, Davis, and Bonner.[5] Since the measurements of Gabbard *et al.* extend only up to a proton energy of 3.0 Mev, we have used the relative cross-section measurements of Bair *et al.*,[4] normalized to the values of Gabbard *et al.*, for higher proton energies. It should be pointed out that the absolute cross section given in a compilation[15] is lower than that of Gabbard *et al.*

[15] Los Alamos Scientific Laboratory Report, La-2014, edited by N. Jarmie and J. D. Seagrave, 1957 (unpublished).

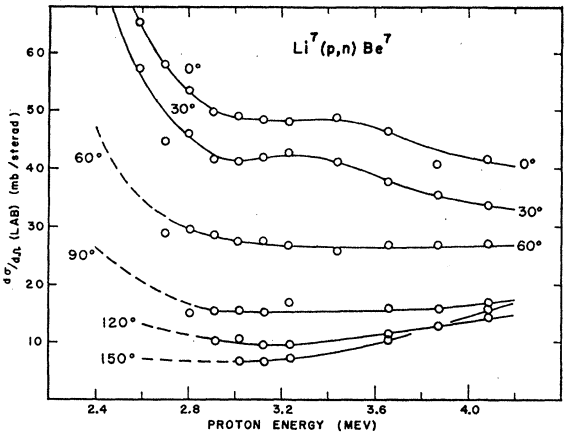

FIG. 4. Differential cross sections of the (p,n) reaction, normalized to the 0° cross section of Gabbard *et al.*[5]

because it was normalized to the results of earlier measurements.[16] Agreement is obtained by multiplying this published curve[15] by the factor 1.35.

The absolute differential cross sections for the (p,n') reaction are plotted as functions of energy in Fig. 3. The errors shown were estimated from uncertainties in the detector efficiency and in the normalization procedure. Errors are $\pm 20\%$ and $\pm 10\%$, respectively, for the two lowest energy points at each angle; for all other points the errors are $\pm 8\%$ in addition to the systematic error in the absolute 0° cross section.

The low-energy extrapolations are derived from the total cross-section measurements of Batchelor and Morrison,[2] assuming isotropy in the center-of-mass system and multiplying by 1.35 to normalize to the work of Gabbard *et al.*[5] Solid dots are the results of Batchelor and Morrison[2] multiplied by 1.35. Agreement with these values in the region of overlap is within quoted errors.

The absolute differential cross sections for the (p,n) reaction are plotted as functions of energy in Fig. 4.

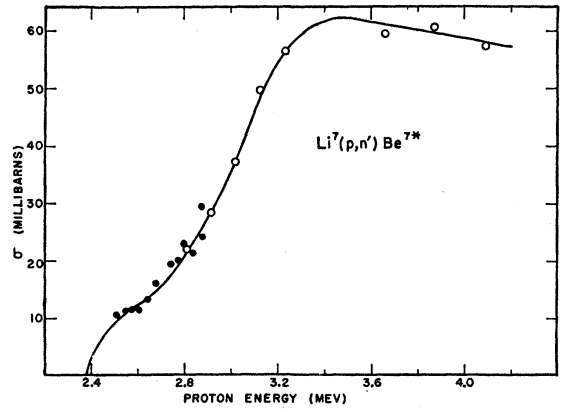

FIG. 5. Total cross section of the (p,n') reaction, obtained by integrating the differential cross sections. Solid dots and the low-energy extrapolation show the results of Batchelor and Morrison.[1,2]

[16] R. Taschek and A. H. Hemmendinger, Phys. Rev. 114, 571 (1959).

Statistical errors are slightly lower than those for the (p,n') reaction because of higher counting rates, and errors due to shifts in efficiency are smaller because of the higher neutron energies. Errors are $\pm 8\%$ for all points.

The total cross section for the (p,n') reaction, shown in Fig. 5, is obtained by integrating the differential cross section over all angles, wherever enough angles were measured. The solid curve above 2.8 Mev is drawn through our data points. Solid dots and the low-energy extrapolation are from the work of Batchelor and Morrison,[2] multiplied by 1.35. The shape of the extrapolation is supported by measurements made at the Argonne National Laboratory[17] of the ratio of the yields of the two neutron groups.

The total cross section for the (p,n) reaction, shown in Fig. 6, is obtained by subtracting the cross section for the (p,n') reaction from the cross section for production of all neutrons, as measured by Gibbons and Macklin.[3] A good check of the experimental results,

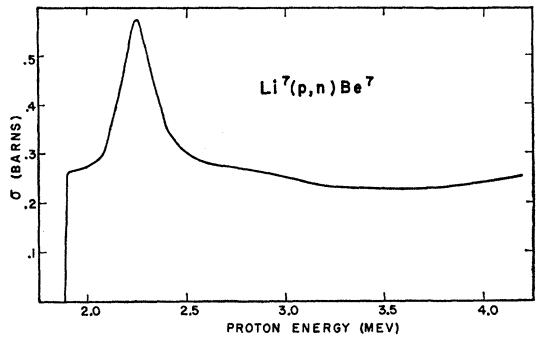

FIG. 6. Total cross section of the (p,n) reaction, calculated by subtracting the (p,n') total cross section from the total cross section of Gibbons and Macklin[3] for production of all neutrons.

as well as an independent check on the normalization, can be obtained by comparing this curve with that obtained by integrating the differential cross section for the (p,n) reaction over all angles; agreement is within $\pm 6\%$.

The angular distributions are plotted, in the center-of-mass-system, in Figs. 7 and 8 for several of the energies measured.

ANALYSIS OF RESULTS

Reactions which may compete in the decay of the compound nucleus Be^8 are alpha-particle emission, gamma-ray emission (proton capture), neutron emission to the ground state or the first excited state of Be^7, and proton emission to the ground state or the first excited state of Li^7. Alpha-particle emission is possible only from states with even spins and parities; generally alpha-particle emission dominates whenever it is allowed, and the contribution of other reactions is negligible. For the energy region under consideration,

[17] Private communication from Dr. A. B. Smith, Argonne National Laboratory.

proton capture is assumed to be negligible in comparison with competing reactions.

The ground states of both Li^7 and Be^7 have $J^\pi=\frac{3}{2}^-$, and the first excited states of Li^7 and Be^7, at 478 kev and 430 kev, respectively, have $J^\pi=\frac{1}{2}^-$. Thus, for reactions of the type (p,n), (p,n'), (p,p), and (p,p'), the orbital angular momenta of the incident and emerging particles are either both even or both odd, and the parity of the state of Be^8 formed is $(-1)^{l+1}$, where l is the orbital angular momentum of the incident proton.

Two levels in Be^8, corresponding to incident proton energies of 1.9 Mev and 2.25 Mev, are known to contribute significantly to the yield of the (p,n) reaction.[18,19] The first of these levels has $J^\pi=2^-$ and a large total width (probably several Mev); the second has $J^\pi=3^+$ and a total width at resonance of 220 kev. For both levels, $\gamma_n^2\simeq 5\gamma_p^2$ where γ_n^2 and γ_p^2 are the reduced widths for neutron and proton emission, respectively. Neither level can contribute significantly to the yield of the (p,n') reaction because decay to the

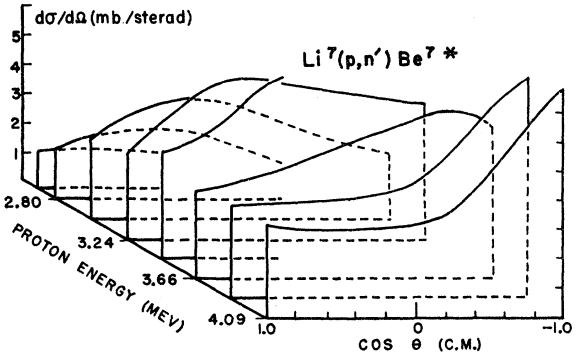

FIG. 7. Angular distributions of the (p,n') reaction for proton energies of 2.70, 2.80, 3.02, 3.24, 3.44, 3.66, 3.88, and 4.09 Mev.

$\frac{1}{2}^-$ level of Be^7 requires outgoing d-wave and f-wave neutrons, respectively, for the resonances at 1.9 Mev and 2.25 Mev, and the barrier penetration at these energies is small.

Two other levels are known in the energy range under consideration, one corresponding to a proton energy of 3.0 Mev,[20] with $J^\pi=2^+$, which decays primarily by alpha-particle emission, and the other corresponding to a proton energy of 2.1 Mev,[18] with $J^\pi=3^-$ (or 3^+), which does not contribute significantly to the yield of the (p,n) reaction and would not be expected to contribute to the yield of the (p,n') reaction because of the high angular momentum required.

Batchelor and Morrison[2] have pointed out that the total cross-section curve for the (p,n') reaction rises sharply with increasing energy near threshold, indicating s-wave neutron emission. The angular distributions for this reaction are nearly isotropic near threshold,[2] in agreement with this assumption.

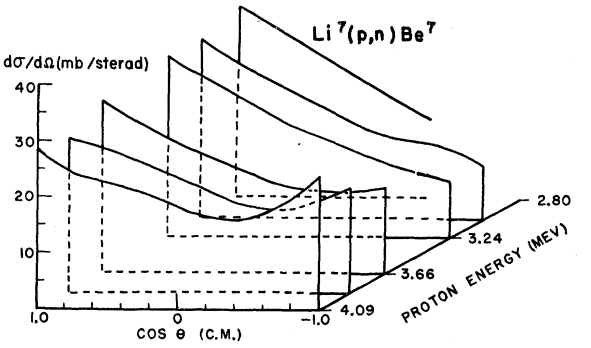

FIG. 8. Angular distributions of the (p,n) reaction for proton energies of 2.80, 3.02, 3.24, 3.66, 3.88, and 4.09 Mev.

Above 2.6 Mev, however, the total cross section rises much more slowly to a maximum near 3.5 Mev, indicating a resonance near 3.5 Mev with p-wave neutrons out and therefore p-wave protons in. Because of the requirements outlined above, this leads to the conclusion that $J^\pi=1^+$. The theoretical cross section, assuming a 1^+ level and using the Breit-Wigner one-level formula, is shown in Fig. 9 (solid line) for a total width at resonance of 1.4 Mev (in the laboratory system), $\gamma_n^2=\gamma_p^2$, $\gamma_{n'}^2=5\gamma_p^2$, and $\gamma_{p'}^2\ll\gamma_p^2$. It was assumed that only one set of channel spins contributes to the resonance. The Coulomb barrier penetration factors were calculated using a nuclear radius $R=1.4A^{\frac{1}{3}}$ fermis.[21]

The assignment $J^\pi=1^+$ is consistent with the shape of the angular distributions for the (p,n') reaction, which have maxima near 90° for proton energies between 3.0 Mev and 3.6 Mev. A choice of channel spins $S_1=1$ (incoming) and $S_2=0$ (outgoing) is necessary to yield a theoretical angular distribution of the form $W=1-\cos^2\theta$, in addition to the isotropic background of the $l_{n'}=0$ resonance near the (p,n') threshold. However, for proton energies near 3.0 Mev, there are

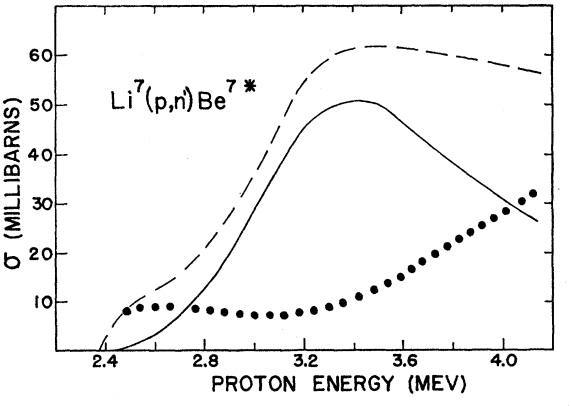

FIG. 9. Cross section of the (p,n') reaction. Dashed line, experimental cross section; solid line, calculated contribution of the resonance at 3.5 Mev; dotted line, difference between experimental and calculated cross sections.

[18] H. W. Newson, R. M. Williamson, K. W. Jones, J. H. Gibbons, and H. Marshak, Phys. Rev. **108**, 1294 (1957).
[19] R. L. Macklin and J. H. Gibbons, Phys. Rev. **109**, 105 (1958).
[20] F. Ajzenberg-Selove and T. Lauritsen, Nuclear Phys. **11**, 1 (1959).
[21] R. F. Christy and R. Latter, Revs. Modern Phys. **20**, 185 (1948).

indications of asymmetry about 90°, indicating interference with a 1^- level near the (p,n') threshold with channel spins $S_1=S_2=1$ for both resonances.

Subtraction of the calculated curve for the 3.5-Mev resonance from the measured cross section (dashed line, Fig. 9) results in a curve (dotted line) which shows that the bulk of the yield of the (p,n') reaction near 3.5 Mev can be ascribed to this resonance. The shape of the $l_{n'}=0$ resonance near the (p,n') threshold is not known exactly, but it is clear that the contribution from this resonance is considerably smaller. All attempts to fit the curve with a choice of $J^\pi=0^-$ have been unsuccessful. Furthermore, the observed asymmetry in the angular distributions for the (p,n') reaction is inconsistent with interference between a resonance below 3.0 Mev with $J^\pi=0^-$ and the resonance at 3.5 Mev.

Hence $J^\pi=1^-$ is the most probable assignment to the $l_{n'}=0$ level, but the large number of possible competing reactions precludes the possibility of fitting the curve exactly. We estimate that the level corresponds to a proton energy of about 2.5 Mev.

Figure 10 shows the calculated contribution to the yield of the (p,n) reaction (solid line) for the resonances at 1.9 Mev and 2.25 Mev,[19] and the resonance at 3.5 Mev described above. The reduced width for neutron emission from the 1.9-Mev resonance is taken to be equal to the Wigner limit as an approximation ($\gamma_n^2>\frac{1}{3}$ the Wigner limit[18]). The maximum contribution from the resonance at 3.5 Mev is 16 mb.

Subtraction of this calculated curve from the measured cross section (dashed line) reveals a peak in the remaining yield (dotted line) at 3.0 Mev with a total width of 1 Mev. This resonance can be fitted approximately by assigning $J^\pi=1^+$, with γ_n^2 several times larger than γ_p^2, $\gamma_{n'}^2\ll\gamma_n^2$, and $\gamma_{p'}^2=\gamma_p^2$. The existence of such a level was first postulated by Newson *et al.*[18] A resonance in the (p,p') reaction[18] at a proton energy of 3.0 Mev and the interference observed in the (p,p) reaction[22] are consistent with this choice of parameters.

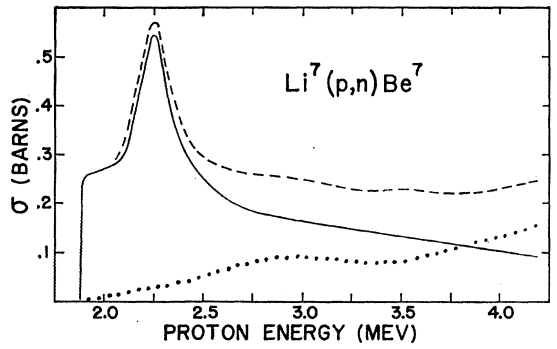

FIG. 10. Cross section of the (p,n) reaction. Dashed line, experimental cross section; solid line, calculated contribution of the resonances at 1.9 Mev, 2.25 Mev, and 3.5 Mev; dotted line, difference between experimental and calculated cross sections.

[22] P. R. Malmberg, Phys. Rev. **101**, 114 (1956).

TABLE I. Levels in Be^8 from Li^7+p.

E_p (Mev)	J^π	Γ (Mev)	Observed reactions	γ_n^2/γ_p^2	$\gamma_{n'}^2/\gamma_p^2$
1.9	2^-	several	(p,n), (p,p), (p,p')	5.2	
2.1	3^-	0.4	(p,γ), (p,p)		
2.25	3^+	0.22	(p,n), (p,p)	5.2	
(2.5)	(1^-)		(p,n')		
3.0	2^+	1.0	(p,α)		
3.0	1^+	1	(p,n), (p,p), (p,p')	(5)	$\ll 5$
3.5	1^+	1.4	(p,n')	(1)	5

Furthermore, the angular distributions of the (p,n) reaction for proton energies near 3.0 Mev are highly peaked in the forward direction. The resonance at 2.25 Mev is too narrow to contribute to this peaking; interference between the 2^- level at the (p,n) threshold and a level corresponding to a proton energy of 3.0 Mev with $J^\pi=1^+$ can result in a term of the form $W=\cos\theta$, in agreement with the observed asymmetry.

The cross-section curves for both neutron groups suggest the presence of a pronounced resonance above 4.1 Mev. The angular distributions of the (p,n') reaction become highly peaked at back angles for proton energies near 4 Mev. Presumably, this is the result of interference between the resonance at 3.5 Mev and a resonance above 4.1 Mev. It is not possible to say, without data at higher energies, whether or not the yield from both groups can be ascribed to a single level in Be^8, corresponding to a proton energy of 5.0 Mev, as suggested by total cross-section measurements.[3]

CONCLUSION

There is strong evidence from the total cross section of the (p,n') reaction, consistent with angular distributions, for a level corresponding to an incident proton energy of 3.5 Mev, with $J^\pi=1^+$ and a width at resonance of 1.4 Mev (in the laboratory system). There is also justification for assuming a level near the (p,n') threshold with $J^\pi=1^-$, on the basis of both angular distributions and total cross sections of the (p,n') reaction. Evidently these two resonances do not contribute greatly to the yield of the (p,n) reaction; presumably there is a 1^+ level corresponding to a proton energy near 3.0 Mev which contributes to the yield of the (p,n) and (p,p') reactions.

The parameters for seven levels within the energy range discussed are summarized in Table I. It should be noted that these levels in Be^8, at an excitation energy of about 20 Mev, are broad and overlapping, and it is by no means certain that the parameters for such resonances can be assigned conclusively.

ACKNOWLEDGMENTS

We would like to thank G. E. Mitchell, R. M. Wilenzick, and Dr. D. R. Tilley for their assistance in taking the data, and Professor H. W. Newson for helpful discussions.